

Sensor and Simulation Notes

Note 391

9 February 1996

CLEARED  
FOR PUBLIC RELEASE  
PL/PA 23 Feb 96

Design of the Low-Frequency Compensation  
of an Extreme-Bandwidth TEM Horn and Lens IRA

M.H. Vogel  
Phillips Laboratory / WSQ  
3550 Aberdeen SE, Kirtland AFB, NM 87117-5776, U.S.A.

on assignment from

TNO Physics and Electronics Laboratory  
P.O. Box 96864, 2509 JG The Hague, NETHERLANDS.

Abstract

The TEM horn and the lens IRA, when radiating an extreme-bandwidth pulse, present, for the low-frequency part of the pulse, an open circuit to the source, which can be a problem. Therefore, a resistive termination has to be connected to the two conductors of the horn. The design of this resistive termination is important, as it significantly affects the low-frequency performance. By routing the currents behind the horn, the associated magnetic dipole moment can be oriented to combine with the electric dipole moment to enhance low-frequency radiation in the forward direction (same direction as the high-frequency radiation) and reduce it in the backward direction.

This paper presents the requirements for the termination, an analytical and a numerical approach to design the termination, as well as several designs that meet the requirements.

## 1. Introduction

Many applications require radiation of a very short (i.e. extreme-bandwidth) pulse of electromagnetic energy out to large distances. These applications include the disruption of electronic equipment, radar target discrimination in a cluttered environment (e.g. targets close to the sea surface or hidden by foliage), radar target identification by means of high resolution (e.g. military vehicles or buried objects), and probing of materials without damaging them. Short pulses for which the ratio between the highest and the lowest frequencies in the spectrum (at the -3 dB points) are of the order of 100:1 without dispersion (i.e. with pulse fidelity) are often desirable. To radiate such an extreme-bandwidth pulse, a TEM horn can be used.

A diagram of a TEM horn is shown in figure 1.1. It consists of a TEM transmission line of almost constant impedance. A lens may be included at the horn aperture to obtain an improvement in the boresight directivity for the high frequencies. In the latter case, it is called a lens impulse radiating antenna (lens IRA or LIRA).

In this paper, we concentrate on the low-frequency behaviour of the TEM horn. As a TEM horn can be modeled as a transmission line, it presents an open circuit for the low-frequency part of the pulse [1]. As a result, a large part of the energy will be reflected towards the source and may damage it. A remedy is to connect a resistive termination to the horn, so that it will no longer act as an open circuit for the low frequencies. Preferably, the resistance of this termination is matched to the impedance of the horn, so that it behaves as a matched load to a transmission line. The physical shape of this resistive termination is important, as it significantly affects the low-frequency performance. This has been pointed out in [2], and will be summarized in the next section.

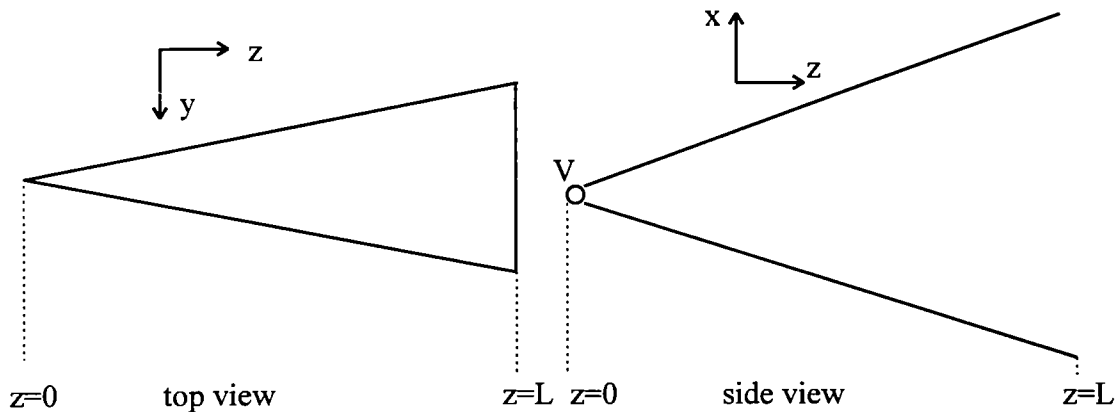


Figure 1.1. TEM horn

## 2. Design Considerations for the Low-Frequency Compensation

In the low-frequency limit, we are dealing with a quasistatic problem. Then, because of the voltage difference between the plates, there will be positive charge on the upper antenna plate and negative charge on the lower plate. As a consequence, the antenna (in combination with the terminating loop) has an electric dipole moment and there is a toroidal electric-field distribution around it. Furthermore, the current that flows through the antenna and the terminating loop gives the antenna (in combination with the loop) a magnetic dipole moment as well, and there is a magnetic field around the antenna, the properties of which are determined by the size and shape of the terminating loop and the magnitude of the current. As was pointed out in [2,3], it is desirable to have the magnitudes and directions of both dipole moments matched in such a way that they combine to orient the low-frequency radiation in the forward direction and cancel the low-frequency radiation in the backward direction.

Consider the three possible designs in figure 2.1. If the resistor is placed near the source, as in figure 2.1A, the electric dipole moment will dominate the magnetic one, and the low-frequency antenna pattern will be toroidal. If the resistor is placed near the horn aperture, as in figure 2.1B, the electric and magnetic dipole moments will, if their magnitudes are matched, combine in such a way that the Poynting vector, for low frequencies, is directed backward. This is of course just the opposite of what we want, as it is in the direction opposite to the high-frequency radiation. The design presented in figure 2.1C reverses the orientation of the current loop, and hence in this case the electric and magnetic dipole moment will, if their magnitudes are matched, combine to direct the Poynting vector for low-frequencies forward. A cardioid antenna pattern will result for these low frequencies, with a null in the backward direction.

With the design presented in figure 2.1C compared to the design without a compensating loop, we can achieve the following:

1. avoidance of reflections back into the source,
2. better directivity for low frequencies,
3. a larger radiation bandwidth.

This will only be achieved when the magnitudes and directions of the electric and magnetic dipole moment are matched. The matching condition, as explained in [2], is

$$\begin{aligned} m_y &= p_x c , \\ m_x &= m_z = 0, \quad p_y = p_z = 0 , \end{aligned} \tag{2.1}$$

in which  $m_x$ ,  $m_y$  and  $m_z$  are the components of the magnetic dipole moment  $\mathbf{m}$  in  $\text{Am}^2$ ,  $p_x$ ,  $p_y$  and  $p_z$  are the components of the electric dipole moment  $\mathbf{p}$  in  $\text{Cm}$ , and  $c$  is the speed of light in  $\text{m/s}$ . We will now discuss the parameters that may be varied to achieve the matching condition.

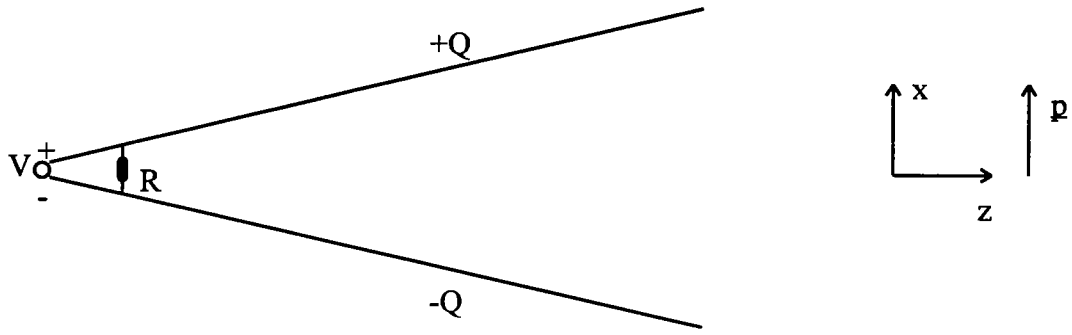


Figure 2.1A. Termination near source connection

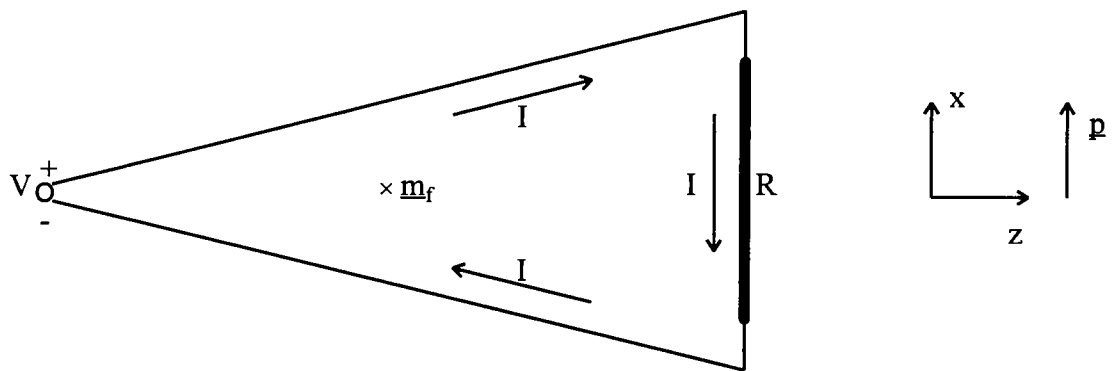


Figure 2.1B. Termination near horn aperture

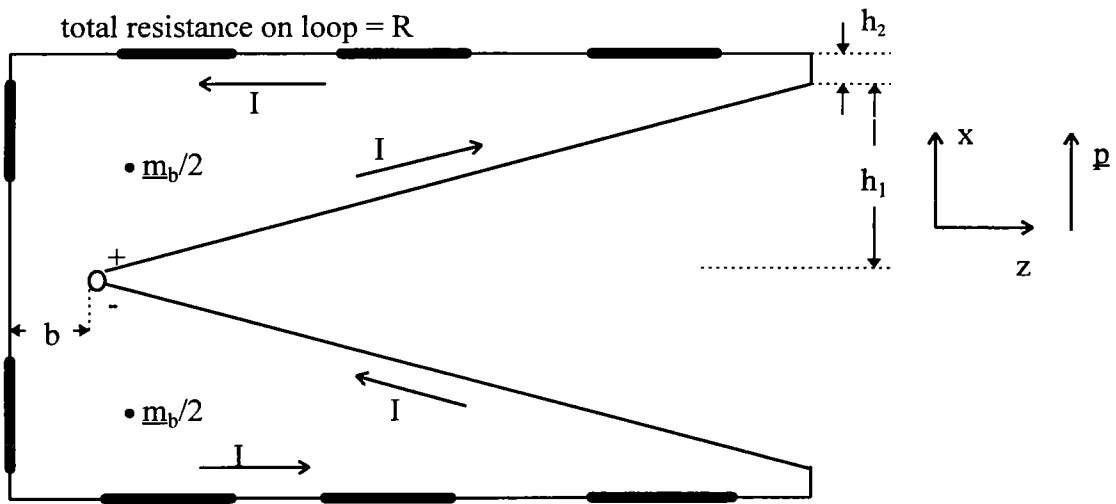


Figure 2.1C. Termination behind horn

Figure 2.1. Possible designs of the resistive termination

The electric dipole moment is determined by the charge distribution in the low-frequency limit, which in turn depends on the size and shape of the entire antenna-loop combination and the voltage distribution on it. We assume that the voltage on the antenna plates as well as the size and shape of the plates are determined by other considerations in the antenna design and cannot be varied freely anymore. The total resistance in the loop has to be equal to the characteristic impedance of the antenna, which also cannot be varied freely anymore. Thus, what can still be varied to change  $p$  are the size and shape of the loop and the distribution of resistors along the loop. The magnetic dipole moment is determined by the magnitude of the current and the area of the loop. The magnitude of the current depends on the voltage and the resistance, which cannot be changed. Thus, what can still be varied to change  $m$  is the area of the loop. Combining the observations on the electric and magnetic dipole moment, we have to design the size and shape of the loop and the distribution of resistors along the loop in such a way that the matching condition is satisfied. Also, we want both moments to be large, in order to maximize the radiated power for low frequencies. The size of the loop should, however, not be much larger than the overall dimensions of the TEM horn, as in most applications the space available for the entire structure is limited.

Consider figure 2.1C, in which, for a rectangular loop shape, some variables are introduced.

From this figure, we conclude that, to optimize our design, we can vary

- $h_2$ , the height above the aperture rim,
- $b$ , the distance behind the apex of the antenna,
- the cross section of the loop, e.g. one or more wires, their radii, or strips with certain widths,
- the distribution of the resistors along the loop.

The parameter  $h_2$  should always be kept small. In some applications, the available space for the antenna will hardly be larger than the antenna itself. The effect of increasing  $h_2$  is an increase in the area of the loop, which means an increase in the magnetic dipole moment. The effect on the electric dipole moment can be positive as well as negative, but at a smaller rate.

The parameter  $b$  should not be large for the same reason as for  $h_2$ , but as we already had to reserve some space behind the antenna for the source, there will usually be some space available for the loop as well. The effect of an increase in  $b$  is an increase in the area of the loop, which means an increase in the magnetic dipole moment. The effect on the electric dipole moment can be positive as well as negative, but at a smaller rate.

As loop cross sections, we have performed calculations on designs with one wire and with two parallel wires, in both cases with variable radii, as well as on strip-like structures. We will present the results in Section 4. For a constant loop area, the variation of the loop cross section doesn't affect the magnetic dipole moment. The way the electric

dipole moment is affected depends on how the total charge on the loop is affected. The effect can be both positive and negative.

The distribution of resistors along the loop doesn't affect the magnetic dipole moment. It does affect the charge distribution, and therefore electric dipole moment. In general, when we move part of the resistors closer to the antenna aperture,  $p_x$  decreases significantly. When we move part of the resistors farther away from the aperture,  $p_x$  increases significantly.

In the next section, we will outline an analytical approach to obtain an antenna design with the desired properties.

### 3. An Analytical Approach to Match the Electric and Magnetic Dipole Moments

In our analytical approach, we assume that the antenna and the compensating loop, as depicted in figure 2.1C, are both very long, so that end effects can be neglected. As a start, we take  $b=0$ , i.e. the loop doesn't extend behind the source. The design procedure then consists of the following steps:

1. Specify the distribution of resistors along the loop and specify  $h_2$ .
2. Knowing the distribution of resistors, solve for the voltage distribution along the loop. The voltage on the upper antenna plate is  $V_0$ , the voltage on the lower antenna plate is  $-V_0$ .
3. Solve for the charge distribution on the entire structure (antenna plates and loop).
4. Knowing the charge distribution, calculate the electric dipole moment  $\underline{p}$ .
5. Knowing the current and the loop shape, calculate  $\underline{m}$  and compare  $\underline{m}$  to  $\underline{pc}$  (cf. (2.1)). If a modification is needed, go back to step 1 and repeat the procedure.

Obviously, the main challenge is in step 3. An efficient method to obtain the charge distribution on a cylindrical structure (a two-dimensional problem) is given in [4,5]. Now, consider the cross section of our antenna+loop structure as given in figure 3.1. The cross section has been taken at an arbitrary location between source and aperture (i.e. arbitrary  $z$ -coordinate). In this figure,  $W$  is the width of the plates at the aperture plane, and  $L$  is the distance between apex and aperture plane (cf. fig. 1.1).

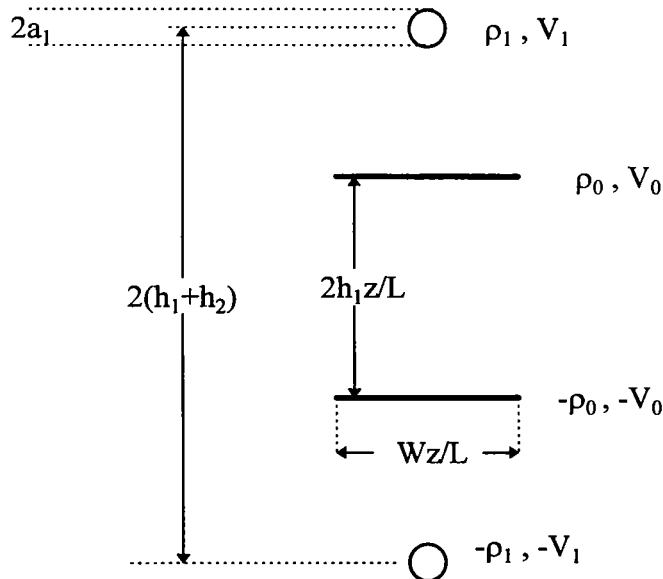


Figure 3.1. Cross section of antenna+loop structure at arbitrary  $z$

Note that, as we have assumed the structure to be very long, we can, for each  $z$ , solve for the charge distribution as if the geometry were two-dimensional. We just need to obtain a relationship between the charge density distribution and the voltage distribution for the two-dimensional case depicted in figure 3.1. The charge density distribution will be a function of  $z$  of course, as the distances between the conductors, the voltages on the loop and the widths of the plates are all functions of  $z$ .

Because of symmetry, the problem reduces to the following equations:

$$\begin{aligned}\rho_1 &= c_{11}V_1 + c_{12}V_0, \\ \rho_0 &= c_{21}V_1 + c_{22}V_0,\end{aligned}\tag{3.1}$$

in which  $\rho_{1,0}$  denotes the charge per unit length on the upper half of the loop or on the upper antenna plate, respectively, and  $V_{1,0}$  denotes the voltages on these structures. All are functions of  $z$ . To obtain the coefficients  $c_{11}$ ,  $c_{12}$ ,  $c_{21}$ ,  $c_{22}$ , we invoke the inverse equations

$$\begin{aligned}V_1 &= d_{11}\rho_1 + d_{12}\rho_0, \\ V_0 &= d_{21}\rho_1 + d_{22}\rho_0.\end{aligned}\tag{3.2}$$

Once matrix  $\underline{D}=(d_{n,m})$  has been found, matrix  $\underline{C}=(c_{n,m})$  can be obtained by taking the inverse of  $\underline{D}$ . To obtain the coefficients of  $\underline{D}$ , we use the relation between voltage and charge density in two dimensions [6]

$$V(\underline{r}_p) = \frac{-1}{2\pi\epsilon_0} \int \rho_s(\ell) \ln|\underline{r}_p - \underline{r}(\ell)|^2 d\ell,\tag{3.3}$$

in which  $\underline{r}_p$  denotes the point of observation,  $\underline{r}(\ell)$  denotes the point on the surface where the surface charge density is given by  $\rho_s(\ell)$ , and  $\ell$  is a local coordinate on the surface (at constant  $z$ ) over which the integration is carried out.

Using (3.3) while making simplifying assumptions about the charge density distribution  $\rho_s(\ell)$  (for constant  $z$ ) over the surface of each conductor, we establish linear relations for each  $z$  between the charge densities  $\rho_1$  and  $\rho_0$  and the voltages  $V_1$  and  $V_0$ , i.e. we have obtained the coefficients of matrix  $D$ . The coefficients of  $C$  are obtained by taking the inverse of  $D$ . The resulting relation between charge densities and voltages is

$$\rho_1(z) = \frac{2\pi\epsilon_0}{\ln(f)\ln(g) - \ln^2(k(z))} (\ln(g)V_1(z) - \ln(k(z))V_0),\tag{3.4a}$$

$$\rho_0(z) = \frac{2\pi\epsilon_0}{\ln(f)\ln(g) - \ln^2(k(z))} (\ln(f)V_0 - \ln(k(z))V_1(z)), \quad (3.4b)$$

in which

$$f = \frac{2h}{a_1}, \quad g = \frac{8h_1}{W}, \quad k(z) = \frac{hL + h_1z}{hL - h_1z}. \quad (3.4c)$$

In (3.4c),  $a_1$  is the radius of the wire,  $W$  is the width of the antenna plate at the aperture,  $h$  is the height of the horizontal section of the wire above the apex of the antenna,  $L$  is the length of the antenna,  $h_1$  is half the vertical dimension of the aperture (at  $z=L$ ). For the entire antenna+loop  $p_x$  is subsequently calculated by means of (3.5):

$$p_x = \int_{z=0}^L \left( 2\rho_0(z) \frac{zh_1}{L} + 2\rho_1(z)h \right) dz. \quad (3.5)$$

We have calculated an expression for  $p_x$  for the case of a uniform distribution of resistors along the loop, i.e. a linear voltage distribution. Unfortunately, the integration in (3.5) can, even in this simple case, not be carried out in closed form. We have split the integral in three separate integrals for small, intermediate and large  $z$ , made appropriate approximations such that the three integrations could be carried out, and have added the results.

We will now give a numerical example. For  $V_0=1.5$  MV,  $Z=240 \Omega$ ,  $L=137$  cm,  $W=50$  cm,  $h_1=50$  cm,  $h_2=10$  cm,  $b=0$ ,  $a_1=2$  cm, we obtain, with a uniform distribution of resistors along the loop,

$$p_x = 28 \mu\text{Cm}, \quad m_y = 7.7 \text{ kAm}^2.$$

Hence,  $p_x$  multiplied by the speed of light  $c$  is equal to  $8.4 \text{ kAm}^2$ , which is 10% larger than  $m_y$ . As our goal is to match  $p_x c$  and  $m_y$ , this result indicates that just a small decrease in  $p_x$  or a small increase in  $m_y$  will give us the desired result.

We can now proceed to adjust  $b$ ,  $h_2$  or  $a_1$  and repeat the process, or we can derive an expression for  $p_x$  resulting from another resistor distribution, and match  $p_x c$  and  $m_y$ . However, the approximations made to obtain this analytical result may be quite crude, especially the assumption of a very long structure and the assumptions concerning the charge density distribution in the directions perpendicular to  $z$ . Therefore, we prefer to proceed with numerical calculations, in which the analytical result obtained thus far will serve as a useful starting point and as a necessary check on the first numerical results.

#### 4. A Numerical Approach to Match the Electric and Magnetic Dipole Moments

As pointed out by Harrington [7], the Method of Moments is very well suited to calculate the charge distribution on an arbitrarily shaped three-dimensional perfectly conducting structure, once the voltages are known everywhere on this structure. In three dimensions, the relation between the electrostatic potential  $V$  at the point of observation denoted by  $\underline{r}_p$  and the surface charge density distribution  $\rho_s(\underline{r})$  on a metal object is given by [7]

$$V(\underline{r}_p) = \iint_{\text{surface}} \frac{\rho_s(\underline{r})}{4\pi\epsilon_0 |\underline{r}_p - \underline{r}|} dS. \quad (4.1)$$

On the antenna and the loop, the voltage distribution is known while the charge density distribution is to be calculated. To this aim, the structure is divided into many planar quadrilateral panels. The wires in the structure are nonplanar, but, as has been proven by King [8], a wire of radius  $a_1$  can be modeled as a strip of width  $4a_1$ . Hence the entire structure can be divided into planar quadrilateral panels. On each panel, the voltage and the charge density are supposed to be constant. The panels can always be made sufficiently small to justify this approximation. When we number the panels 1 to  $N$ ,  $N$  being the total number of panels, we have for the voltage on each panel the following equation:

$$V_n = \sum_{m=1}^N L_{nm} \rho_{s,m}, \quad (4.2)$$

where, for combinations of panels that are not very close,

$$L_{nm} = \frac{A_m}{4\pi\epsilon_0 R_{nm}}, \quad (4.3)$$

in which  $A_m$  is the area of panel  $m$  and  $R_{nm}$  is the distance between the centers of panels  $n$  and  $m$ . The self term for  $m=n$  is given by [7]

$$L_{nn} = \frac{0.282 \sqrt{A_n}}{\epsilon_0}. \quad (4.4)$$

For panels close together, special measures have to be taken, such as a further subdivision of the panels. Finally, a matrix equation results:

$$\underline{V} = \underline{L} \underline{\rho}_s, \quad (4.5)$$

where  $\underline{V}=(V_n)$ ,  $\underline{L}=(L_{nm})$ ,  $\underline{\rho}_s=(\rho_{s,m})$ , in which  $\underline{\rho}_s$  is unknown. The matrix equation is solved by LU-decomposition.

As a check on the correctness of the software, we have applied the Method of Moments to a very long TEM horn with compensating loop, as for this case the analytical

and numerical results should agree. Indeed, for a 10 meter antenna+loop the results agree within 10%, which gives confidence in the correctness of the computer program. For the 1.37 meter antenna+loop, the electric dipole moment, as calculated with the Method of Moments (MoM), turns out to be about 30% larger than the analytical prediction. Apparently, the approximations made in the analytical approach are too crude indeed for such a not-very-long antenna. Therefore, in order to make the final design, we will rely solely on the numerical results, the correctness of which has been demonstrated for the 10 meter antenna. For the 1.37 meter antenna+loop, the characteristic linear dimension of the panels in the antenna and in the loop is 5 cm, with a maximum of 9 cm. The maximum linear dimension of the panels in the ground plane (to be introduced later) is 12 cm. Doubling the number of panels typically changes the calculated value for  $p_x$  by 3%.

Note that the antenna, as depicted in figure 2.1C, is symmetrical in the vertical direction. Therefore, a ground plane ( $V=0$ ) can be introduced and the lower part of the antenna+loop omitted. The subsequent calculations have been performed for an asymmetrical antenna with a finite ground plane (fig. 4.1), the reason being that the antenna will actually be built with a finite-sized ground plane. The size and shape of the ground plane provide extra variables in the antenna design. In all cases, we choose its minimum width to be 0.5 m at  $z=-0.25$  m, and its maximum width to be 1.5 m. The extension of the ground plane in the positive  $z$ -direction is kept as a variable. This mainly influences  $p_z$ , which we assume to satisfy the condition  $p_z=0$  when its calculated absolute value is less than  $0.2 \mu\text{Cm}$ . All calculations with the finite-sized ground plane have been performed subject to the condition that the total charge on the entire structure be zero.

We start with the case where the compensating loop consists of one wire (figure 4.1). The final design for this case, which has resulted after several numerical experiments, has a uniform distribution of resistors along the entire wire (including the vertical sections). Further,  $h_2=2.5$  cm (this means the loop hardly takes more space in the vertical direction than the antenna itself),  $b=15$  cm (this means the loop extends 15 cm behind the source, which is usually no problem), and  $a_1=1$  cm (this means the wire is not very thin, which is good because it has to conduct currents of 12.5 kA, though in very short pulses). The ground plane extends to  $z=1.65$  m. For this design,  $p_x=19 \mu\text{Cm}$  and  $m_y=5.7 \text{ kAm}^2$ , while the other components are zero. Hence, the matching condition (2.1) has been satisfied.

The sensitivity of the result to variation in some parameters is illustrated by the following examples:

When  $h_2=5$  cm instead of 2.5 cm,  $p_x$  increases by 3% while  $m_y$  increases by 8%.

When  $b=22.5$  cm instead of 20 cm,  $p_x$  increases by 1% while  $m_y$  increases by 3%.

When  $a_1=2$  cm instead of 1 cm,  $p_x$  increases by 2% while  $m_y$  remains constant.

When the resistors are distributed uniformly over the horizontal section of the loop only, while the vertical section is a bare wire,  $p_x$  decreases by 9 % while  $m_y$  remains constant.

When the ground plane extends to  $z=1.75$  m instead of  $z=1.65$  m,  $p_z=3 \mu\text{Cm}$  while  $p_x$  decreases by 1%.

We proceed with the case where the compensating loop consists of two wires (figure 4.2). The reason for making a two-wire design is that these will have their attachment points closer to the regions of maximum current density on the antenna plates, and are therefore expected to give a better performance for part of the low-frequency spectrum. In the final design for this case the wires are 25 cm apart, while again  $h_2=2.5$  cm,  $a_1=1$  cm, and the resistors are uniformly distributed. The loop now extends 20 cm behind the source (i.e.  $b=20$  cm), and the ground plane extends to  $z=1.60$  m. For this design,  $p_x=20 \mu\text{Cm}$  and  $m_y=6.0 \text{ kAm}^2$ , while  $p_y$ ,  $p_z$ ,  $m_x$ , and  $m_z$  are zero. Hence, the matching condition (2.1) has again been satisfied.

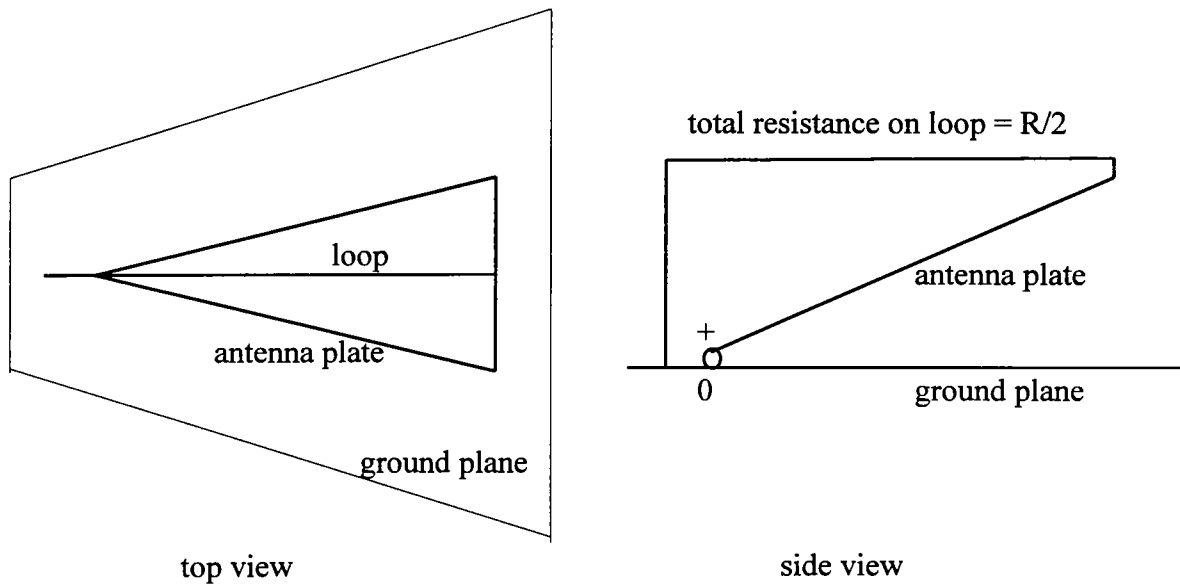


Figure 4.1. TEM horn with one-wire compensating loop

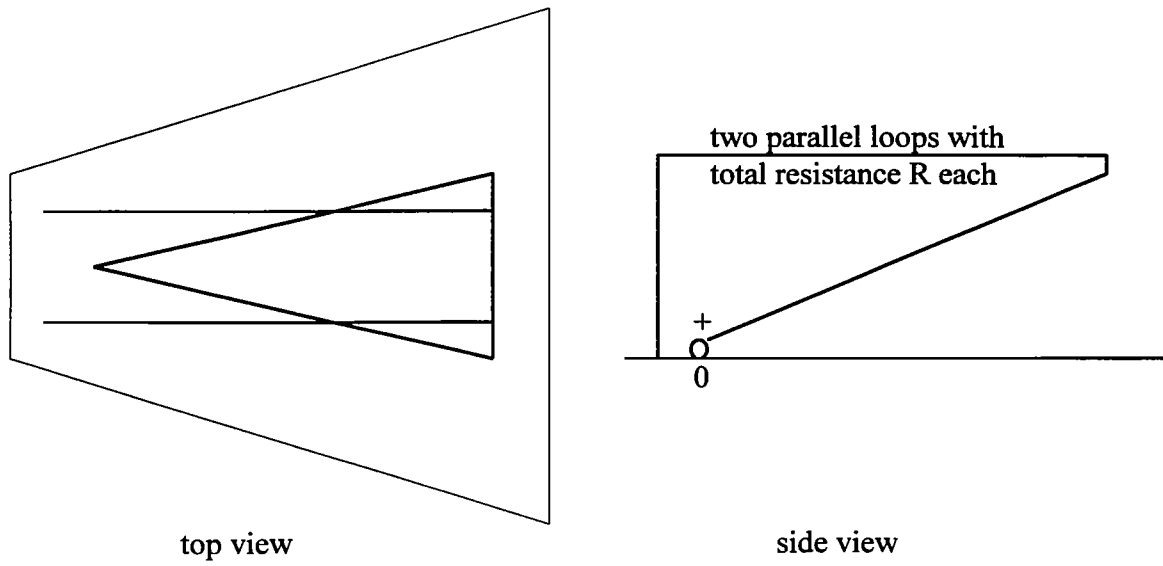


Figure 4.2. TEM horn with two-wire compensating loop

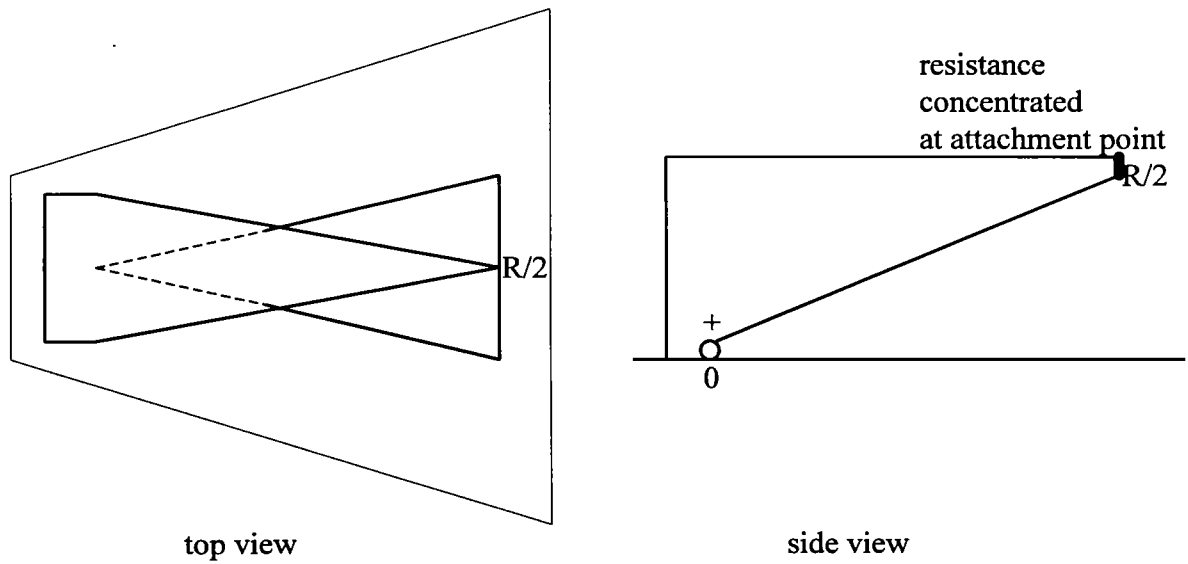


Fig. 4.3. TEM horn with one-triangle compensating loop

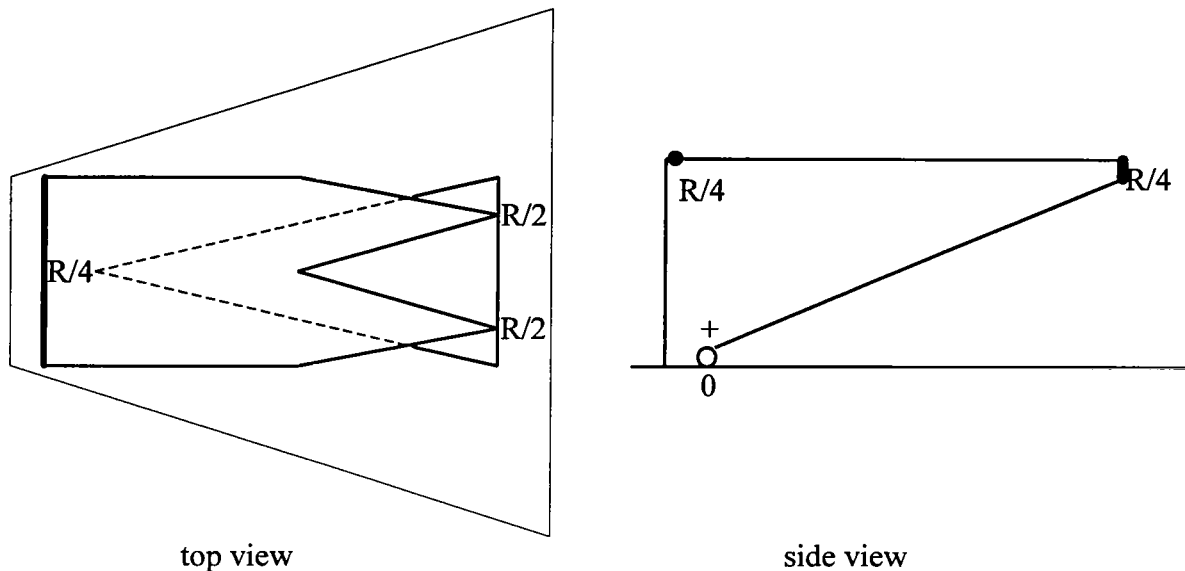


Figure 4.4. TEM horn with two-triangle compensating loop

At this point, we have two designs for the low-frequency compensation of the TEM horn that are both easy to build and that both satisfy all requirements for the low frequencies. For the intermediate and higher frequencies however, note that the fields associated with the charges in the loop and on the plate side facing the loop will radiate in unwanted directions. It is desirable to have a loop design that suppresses the radiation of the TEM fields above the TEM horn. This observation leads us to the design depicted in figure 4.3. We call it the TEM horn with the one-triangle compensating loop.

The idea behind this design is as follows. Fields propagating forward in the space between the antenna plate and the loop will in this design be propagating in a structure that looks like a *receiving TEM horn* with a ground plane. With a matched load at the end (i.e. at the attachment point), their energy will be dissipated in the resistor. A  $120 \Omega$  resistor is a matched load for this case, which is exactly the total resistance required in the loop. Hence, in this case there are no further resistors along the loop; all resistance is concentrated in the attachment point. The voltage along the loop is zero.

With  $b=20$  cm and  $h_2=2.5$  cm, as before, we obtain  $p_x=9.5 \mu\text{Cm}$ , hence  $p_x c=2.8 \text{ kAm}^2$ . Again,  $m_y=6.0 \text{ kAm}^2$ , as neither the current nor the area of the loop has changed. Hence we are far from satisfying the matching condition  $p_x c=m_y$ . The reason is that by bringing all resistance as far forward as possible, we are allowing a significant negative charge on the loop, resulting in a low electric dipole moment. We cannot avoid this by moving the resistors, as all resistance has to be concentrated in the attachment point in order to act as a matched load. Making the loop narrower at the back, so that its negative

contribution to the electric dipole moment diminishes, will not help. In the limit of a very narrow loop, we end up with a wire with all resistance concentrated at the attachment point. From the one-wire design we know that this will still have a far too small electric dipole moment. Hence, we cannot use the one-triangle design.

An alternative design, in which the idea of the matched load can be used as well, is depicted in figure 4.4. Now there are two attachment points on the antenna plate. We call this the TEM horn with the two-triangle compensating loop. Note that radiation traveling in the space between an antenna plate and the loop will still encounter, in the frontal section, a structure that looks like a receiving TEM horn with a ground plane. In each attachment point, the matched load is provided by a  $120 \Omega$  resistor. An important difference with the previous design is that we now have some resistance left to place along the loop at will! Two parallel  $120 \Omega$  resistors form together a  $60 \Omega$  resistor, and we have another  $60 \Omega$  left to place along the loop. We can use this freedom to satisfy the matching condition. It turns out that this is achieved with  $b=10$  cm,  $h_2=2.5$  cm, and with the  $60 \Omega$  placed at the point where where the loop makes an angle (as indicated in the figure). Further, the ground plane extends to  $z=1.75$  m. In this design,  $p_x=18 \mu\text{Cm}$  and  $m_y=5.4 \text{ kAm}^2$ .

## 5. Conclusion

We have presented several designs for a low-frequency compensated TEM horn which does not reflect low-frequency radiation towards the source and which, for the lowest frequencies, does not radiate a toroidal pattern but a cardioid pattern in the forward direction. The compensating loop can be achieved with one or two wires or with adequately shaped plates, with the appropriate distribution of resistors along it. The TEM horn with the two-wire compensating loop is expected to have a better performance than the horn with the one-wire loop for a part of the low-frequency spectrum. The TEM horn with the two-triangle compensating loop has all the virtues of the TEM horn with the two-wire compensating loop, while it is expected to have a better directivity for the intermediate and higher frequencies. Therefore, we have chosen this design to be fabricated and tested. Its properties for the entire frequency spectrum will be the subject of further research, both experimental and computational.

## Acknowledgement

The author wishes to thank the TNO Physics and Electronics Laboratory for giving him the opportunity to conduct this research at the Phillips Laboratory, Dr. C.E. Baum (Phillips Laboratory) for valuable discussions, and Lt.Col. Dr. D.T. McGrath (Phillips Laboratory) for providing most of the software.

## References

- [1] E.G. Farr and C.E. Baum, "A Simple Model of Small-Angle TEM Horns", *Sensor and Simulation Note* 340, May 1992.
- [2] C.E. Baum, "Low-Frequency Compensated TEM Horn", *Sensor and Simulation Note* 377, January 1995.
- [3] C.E. Baum, "Some Characteristics of Electric and Magnetic Dipole Antennas for Radiating Transient Pulses", *Sensor and Simulation Note* 125, January 1971.
- [4] J.C. Clements, C.R. Paul and A.T. Adams, "Computation of the Capacitance Matrix for Systems of Dielectric-Coated Cylindrical Conductors", *IEEE Trans. Electromagnetic Compatibility*, vol. 17, no.4, pp. 238-248, November 1975.
- [5] C.R. Paul and A.E. Feather, "Computation of the Transmission-Line Inductance and Capacitance Matrices from the Generalized Capacitance Matrices", *IEEE Trans. Electromagnetic Compatibility*, vol. 18, no. 4, pp. 175-183, November 1976.
- [6] W.R. Smythe, *Static and Dynamic Electricity*, Third Edition, Chapter 4, Hemisphere Publishing Corporation (Taylor and Francis Group), ISBN 0-89116-917-2, 1989.
- [7] R.F. Harrington, *Field Computation by Moment Methods*, First Printing, Chapter 2, Macmillan Company, LCCCN 68-10184, 1968.
- [8] R.W.P. King, *The Theory of Linear Antennas*, Chapter I-7, Harvard University Press, LCCCN 56-5354, 1956.